

Toxicology Research

Accepted Manuscript



This is an *Accepted Manuscript*, which has been through the Royal Society of Chemistry peer review process and has been accepted for publication.

Accepted Manuscripts are published online shortly after acceptance, before technical editing, formatting and proof reading. Using this free service, authors can make their results available to the community, in citable form, before we publish the edited article. We will replace this *Accepted Manuscript* with the edited and formatted *Advance Article* as soon as it is available.

You can find more information about *Accepted Manuscripts* in the [Information for Authors](#).

Please note that technical editing may introduce minor changes to the text and/or graphics, which may alter content. The journal's standard [Terms & Conditions](#) and the [Ethical guidelines](#) still apply. In no event shall the Royal Society of Chemistry be held responsible for any errors or omissions in this *Accepted Manuscript* or any consequences arising from the use of any information it contains.

***miR-122* plays an important role in Ochratoxin A-induced hepatocyte
apoptosis *in vitro* and *in vivo***

Liye Zhu^a, Tao Yu^a, Xiaozhe Qi^a, Bo Yang^a, Lei Shi^a, Haoshu Luo^b, Xiaoyun He^{a, c},

Kunlun Huang^{a, c}, Wentao Xu^{a, c, *}

^aCollege of Food Science and Nutritional Engineering, China Agricultural University, Beijing,
China, 100083

^bCollege of Biological Sciences, China Agricultural University, Beijing, China, 100083

^cThe Supervision, Inspection and Testing Center of Genetically Modified Organisms, Ministry of
Agriculture, Beijing, China, 100083

Running Title: *miR-122* regulates OTA-induced hepatocyte apoptosis

*Corresponding author

Address: College of Food Science and Nutritional Engineering, China Agricultural University, No.
17 Tsinghua Donglu, Beijing, China, 100083.

Fax/Phone: (8610)62738793; E-mail: xuwentao@cau.edu.cn

Number of figures: 7

Number of tables: 3

Number of figures in color: 2

Table of contents entry

We compared the OTA hepatotoxicity *in vivo* and *in vitro*.

miR-122 regulated *CCNG1/p53* pathway in OTA-induced hepatocyte apoptosis.

miR-122 regulated *Bcl-w/caspase-3* pathway in OTA-induced hepatocyte apoptosis.

Abbreviations

OTA: ochratoxin A

TUNEL: TdT-mediated Dntp nick end labeling

CCK-8: Cell Counting kit-8

AFB1: aflatoxins B1

HCC: hepatocellular carcinoma

HCV: hepatitis C virus

DMEM: Dulbecco's Modified Eagle's Medium

GMOs: genetically modified organisms

PI: propidium iodide

SD: standard deviation

NC: negative control

LDH: lactate dehydrogenase

AST: aspartate transaminase

IC₅₀: half maximal inhibitory concentration of a substance

MMP: mitochondrial membrane potential

IAP: inhibitor-of-apoptosis

Abstract

OTA can induce hepatotoxicity. Our previous research has shown that miRNAs play important roles in the OTA-induced hepatotoxicity. And *miR-122* is the most abundant miRNA in the liver and involved in diverse biological processes. This study was performed to clarify the role of *miR-122* in OTA-induced hepatotoxicity. The expression levels of *miR-122* and the target genes were quantified by real-time PCR. The OTA-induced apoptosis of hepatocyte and HepG2 cells was evaluated using TUNEL kit, CCK-8 kit, flow cytometer and Hoechst 33342. *miR-122* was inhibited in HepG2 cell. The results revealed that OTA affected rat hepatocyte apoptosis. *miR-122* decreased at 4 weeks but increased at 13 weeks in OTA-treatment livers, and increased in OTA-treatment HepG2 cells; And the mRNA levels of *CCNG1* and *Bcl-w* increased at 4 weeks and decreased at 13 weeks in the high-dose OTA-treatment groups and decreased in HepG2 cells. The apoptosis of HepG2 cells displayed a dose-related increase with OTA. However, the inhibition of *miR-122* greatly reduced OTA-induced apoptosis. *p53* decreased *in vivo* and *in vitro*. *miR-122* is a primary effector of OTA-induced hepatocyte apoptosis through the *CCNG1/p53* pathway and *Bcl-w/caspase-3* pathway *in vivo* and *in vitro*. And *miR-122* plays an important role in OTA-induced hepatotoxicity.

Key words: *miR-122*; Ochratoxin A; Hepatotoxicity; Cell apoptosis; *In vivo*; *In vitro*

Introduction

Ochratoxin A (OTA) is a secondary fungal metabolite produced by molds.¹ OTA displays extensive toxicity, including hepatotoxicity, nephrotoxicity, genotoxicity, and teratogenicity.² Previous studies have shown that the liver is one of the major target organs of OTA-induced toxicity. The liver is a vital metabolic regulation organ.³ The mechanisms of OTA action in the liver are controversial and thus warrant further study.

miRNAs are a type of endogenous, conserved, non-coding small RNAs. The length is 20~25 nucleotides. miRNAs are involved in many biological processes. miRNAs can regulate the target genes via post-transcriptional regulation of mRNA translation and stability. Studies have suggested that some fungal toxins resulted in toxicities based on the regulation of miRNAs expression, such as OTA and AFB1.⁴⁻⁷ A new avenue to understand OTA-induced hepatotoxicity is worthy to study.

In our previous studies, we treated F344 male rats with OTA and analyzed the expression levels of miRNAs using multiple omics profiling technologies. We found an abnormal expression of some miRNAs.^{6, 8} Among them, *miR-122* is the most abundant miRNA in the liver, which expressed in the developing liver and at high level in the adult liver. *miR-122* constitutes approximately 70% of all of the miRNAs in the liver,⁹ which appears to correlate with a key role in various functions in normal and diseased livers. The most well-known function of *miR-122* in the mammalian liver is to regulate lipid and cholesterol metabolism.¹⁰ *miR-122* is involved in cancer cell metabolism, apoptosis, and transfer and also considered to be a tumor suppressor in the liver.¹¹ Previous research indicated that *miR-122* was significantly downregulated in 70% of human and mouse hepatocellular carcinomas. Furthermore, another investigation showed that

miR-122 may be a biomarker for the liver toxicity of AFB1,⁴ one of the well-known hepatotoxic mycotoxins. Additionally, *miR-122* was shown to regulate the target gene *CCNG1*, and an inverse relationship between *miR-122* and *CCNG1* was observed in HCC.¹² The regulation of *p53* by *CCNG1* results in cell survival.¹³ Also, a target gene of *miR-122*, *Bcl-w*, promotes cell survival in HCV.^{14, 15} Until now, few studies have reported how OTA regulates miRNAs and results in hepatotoxicity. And the relationship between *miR-122* and hepatotoxicity induced by OTA also has not been reported.

Therefore, our study aimed to investigate the relationship between the OTA-induced hepatotoxicity and the aberrant expression of *miR-122* using *in vivo* and *in vitro* models.

Results and Discussion

OTA affected rat hepatocyte apoptosis

In our previous study, we reported that the serum biochemical indexes were higher at 13 weeks in the low- and high-dose livers compared to the controls.¹⁶ LDH and AST mRNA levels at 13 weeks were lower in the high-dose compared to control rats, while at 4 weeks, LDH and AST were not significantly different. Because LDH and AST could reflect liver damage, this result suggests that liver damage was more severe in the high-dose group at 13 weeks compared to the animals OTA-treated for 4 weeks.¹⁶ Based on the changes of physicochemical indexes, we selected 4 weeks and 13 weeks as the critical time points to analyze OTA-induced hepatotoxicity *in vivo*.

In low- and high-doses groups, hepatocyte apoptosis had a dose-dependent with OTA. A significant decrease of hepatocyte apoptosis at 4 weeks compared to the control group (Fig. 1A). At 13 weeks, hepatocyte apoptosis significantly increased in a dose-dependent manner. The green

fluorescent signal indicated the positions of apoptotic cells (Fig. 1B). The results indicated that the hepatocyte apoptosis had a different relationship with the OTA-treatment doses at different time points.

Dose-dependent OTA-induced HepG2 cell apoptosis

HepG2 cell viability was detected using the CCK-8. The treatment with different doses of OTA leads to a decrease in HepG2 cell viability (Fig.2A). The cell survival rates appeared significantly reduced with the treatment of 5 μM OTA ($p < 0.05$). The IC_{50} of OTA for a 24 h treatment of HepG2 cells was approximately 50 μM (Fig. 2A).

Previous reports suggested that OTA can trigger programmed cell death (apoptosis) and influence the apoptotic signaling pathways.¹⁷⁻¹⁹ In our research, HepG2 cell apoptosis was detected using flow cytometry. The result clearly showed that the percentage of apoptotic cells increased with OTA treatment in a dose-dependent manner. The significant difference was at 20 μM OTA ($p < 0.05$) (Fig. 2B).

To further reflect the cytotoxicity of OTA, the nucleus and apoptotic body formation was detected. The results revealed that HepG2 cells treated with 20 μM OTA stained deep blue compared to the untreated cells. Additionally, the OTA-treated cells displayed a shriveled nucleus, a marker of apoptosis, while the control group did not. Moreover, we can clearly observe the condensation, chromatin marginalization and fragmentation of nuclear chromatin (Fig. 2C). These results all suggest that treatment with 20 μM OTA leads to significant apoptosis in HepG2 cells ($p < 0.05$).

OTA induced changes in the expression of *miR-122* in the liver and in HepG2 cells

In recent studies, to the research of the mechanisms of toxication, microRNAs provided a new

perspective. Our laboratory has previously used transcriptomic and proteomic *in vivo* analysis to explore the roles of miRNAs in OTA-induced early hepatotoxicity.⁸ There are sufficient evidences supporting that the aberrant expression of *miR-122* was found in many hepatic diseases.²⁰⁻²² Based on these findings, we chose to explore the role of *miR-122* in the OTA-induced hepatotoxicity.

The expression of *miR-122* in the livers of rats treated with OTA at 4 weeks and 13 weeks were detected. At 4 weeks, *miR-122* was lower in both the low-and high-dose animals compared to the controls ($p < 0.05$) (Fig. 3A). In contrast, *miR-122* was significantly higher in both the low-and high-dose groups compared to the controls at 13 weeks ($p < 0.05$) (Fig. 3A). The results identified that the expression of *miR-122* at different time and dose points were different *in vivo*.

In HepG2 cells, we discovered that 20 μ M OTA can lead to the significant apoptosis of HepG2 cell; however, the treatment affected the signaling pathway. After the treatment of HepG2 cells with 20 μ M OTA, the expression of *miR-122* was significantly upregulated ($p < 0.05$) compared to the control group (Fig. 3B).

miR-122 was downregulated at 4 weeks and upregulated at 13 weeks *in vivo*. Additionally, *miR-122* was upregulated *in vitro*. The apoptosis increased with the upregulation of *miR-122* induced by OTA *in vivo* and *in vitro*. Some studies have reported that the upregulation of *miR-122* can inhibit cell proliferation and promote apoptosis. In cancer cells, the antitumor activity of Ad-miR-122 was most likely due to the induction of apoptosis.²³ And in *Pax-8*^{-/-} mice, the upregulation of *miR-122* influenced cell viability and regulated the expression of apoptotic genes.²⁴ The overexpression of *miR-122* can induce cell cycle arrest and result in tumorigenicity.²⁵ Lian *et al.* reported that in the carcinogenesis of renal cancer, *miR-122* was upregulated by the *P13K/Akt* signaling pathway.²⁶

OTA induced changes in the expression of *CCNG1/p53* in the liver and in HepG2 cells

In the liver, *CCNG1*, a target gene of *miR-122*, was detected. *CCNG1* was discovered as a member of the cyclin family, a protein family that regulates the cell cycle. *CCNG1* was potently elevated in the high-dose group ($p < 0.05$) compared to the control group at 4 weeks, while its level significantly declined ($p < 0.05$) in the high-dose group at 13 weeks (Fig. 4A). *p53* is regarded as one of the most important tumor suppressor genes and the downstream genes of *CCNG1*. In our study, *p53* was significantly decreased at 4 weeks and 13 weeks in the high-dose group compared to the control groups ($p < 0.05$) (Fig. 4B).

In HepG2 cells, the results indicated the downregulation of *CCNG* (Fig. 4C). The reduced levels of *CCNG1* reflected the altered functional levels of cellular *miR-122*. To verify the signaling pathway, *p53* was determined respectively. *p53* was significantly upregulated in the treatment group compared to the control group ($p < 0.05$) (Fig. 4D). These results are in agreement with the group treated in vivo partly.

OTA treatment affected the expression of *CCNG1*. In the current study, *CCNG1* was higher after 4 weeks and lower after 13 weeks of treatment in the high-dose group *in vivo*. Additionally, *CCNG1* was decreased in HepG2 cells after OTA-treatment. Consistent with the previous report, acute alcohol treatment induced *miR-122* up-regulated and decreased *CCNG1* in Huh-7.5 cells.²⁷ In our study, *p53* was lower in the high-dose group after 4 weeks and 13 weeks of treatment *in vivo*, and also was increased *in vitro*. *CCNG1* and *p53* display a feedback relationship.²⁸ In HCC, *miR-122* influenced the activity of *p53* through the regulation of *CCNG1*, resulting in a lower survival of HCC-derived cell lines.¹³ *miR-122* can interrupt the interaction between *CCNG1* and *p53*, which can favor carcinogenesis.²⁹ Studies also have indicated that *p53* can inhibit tumor cell

proliferation via the induction of DNA damage and cell cycle arrest that then induces the production of *CCNG1*.³⁰ Kato *et al.* found that in a murine erythroleukemic cell line, *p53-CCNG1-COX II* involved in inducing cell apoptosis.³¹ In our study, at 13 weeks, OTA leads to the downregulation of *p53*, which may not occur through the *miR-122/CCNG1* pathway alone, as an increase in the level of *p53* via *miR-122* regulation of *p53/Akt* signaling can induce apoptosis in cutaneous T-cell lymphoma.³² In human gastric epithelium GES-1 cells, OTA treatment can increase *p53* expression.³³ This finding is in agreement with our results *in vitro*. Because hepatocarcinogenesis always follows hepatocyte apoptosis and regeneration.³⁴ These results may also indicate that OTA may induce hepatocellular carcinoma after long-time treatment by regulating the expression of *miR-122* and affecting the *CCNG1/p53* pathway.

OTA induced changes in the expression of *Bcl-w/Caspase-3* in the liver and in HepG2 cells

In vivo, the expression of *Bcl-w*, *miR-122* target gene, was significantly increased at 4 weeks and decreased at 13 weeks ($p < 0.05$) in the high-dose OTA group (Fig. 4A). *Caspase-3*, a member of caspase family, is a predictor of apoptosis. We detected *caspase-3* increased at 4 weeks and decreased at 13 weeks in the high-dose animals (Fig. 4B).

In HepG2 cells, *Bcl-w*, was also determined. The expression level of *Bcl-w* decreased after OTA treatment ($p < 0.05$) (Fig. 4C). And *caspase-3*, the downstream genes of *Bcl-w*, decreased significantly in the treatment group compared to the control group ($p < 0.05$) (Fig. 4D). These results are also in agreement with the group treated for 13 weeks.

Bcl-w is an anti-apoptotic gene of the *Bcl-2* family. And *caspase-3* is a key protein that is involved in the apoptosis. They all existed in mitochondria. OTA can induce apoptosis via regulating the mitochondrial pathway.³⁵ And *miR-122* is also a regulator of the mitochondrial

metabolic gene network.²¹ The mitochondrial pathway is regulated by the *Bcl-2* family.³⁶ *miR-122* can downregulate the expression of *Bcl-w* in HepG2 cells and result in the apoptosis of the HCC-derived cell lines by downregulating the *Bcl-w/Bax* ratio.¹⁵ The treatment with *miR-122* mimetics or *miR-122* inhibitor affects the activity of *caspase-3* in H9C2 myocytes.²⁴ And OTA can induce the activities *caspase-3* and result in the apoptosis of neuronal cells accompanied by the disappearance of the MMP.³⁷ When the MMP collapses, cytochrome c is released into the cytosol and binds to *Apaf-1*, resulting in the recruitment of pro-caspases, which further activates the effector caspases. In our study, *Bcl-w* and *caspase-3* were significantly downregulated at 13 weeks in high-dose group *in vivo* and *in vitro*. While the apoptosis is induced compared to the control group. Consistent with this result, OTA can affect apoptosis by influencing *caspase-3* and *Bcl-2* in HKC cells.³⁸ *Caspase-3* was decreased in HEK293 cells after the OTA treatment.³⁹ In agreement with our result, the inhibition of *caspase-3* may be affected by the inhibitor-of-apoptosis (IAP) family of genes, which regulate apoptosis, block the activity of procaspase-9 induced by cytochrome c, and further prevent the activity of *caspase-3*; however, IAPs cannot prevent the activity of *caspase-8*.^{40, 41} These findings suggest that the OTA-induced apoptosis in the liver and HepG2 cells resulted from the abnormal expression of *miR-122* and the disturbance of the mitochondrial pathway, which resulted in the hepatotoxicity.

***miR-122* inhibitor relieved HepG2 cell apoptosis induced by OTA**

The inhibition efficiency of the *miR-122* inhibitor was detected. There was no difference between the control group (CK) and the inhibitor-negative control group (NC). However, the expression of *miR-122* was decreased with an increase in the concentration of the *miR-122* inhibitor. According to the results, 50 nM inhibitor was confirmed to be the optimal concentration.

Compared to the negative control, there was a significance difference ($p < 0.05$) (Fig. 5A). The inhibition efficiency was approximately 41% compared to the inhibitor-negative group.

After the HepG2 cells were transfected with 50 nM inhibitor, the cells were analyzed for the presence of apoptosis after OTA treatment. The results showed that cell apoptosis was significantly reduced in the inhibitor group compared to the negative group ($p < 0.05$) both treated with 20 μ M OTA. Apoptosis in the cells treated only with the inhibitor did not significantly differ compared to the negative group (Fig. 5B). Additionally, in the group transfected with the inhibitor and also treated with OTA, the apoptotic cells were significantly decreased compared to the inhibitor-negative group ($p < 0.05$).

Hoechst 33342 was used to further observe the apoptosis of HepG2 cells. In Figure 5C, we can clearly observe that the cells, which were only treated with OTA, were markedly more apoptosis than the other groups. Moreover, after OTA treatment, the apoptotic cells were significantly decreased with inhibitor treatment than by inhibitor-negative treatment ($p < 0.05$). The deep blue staining appeared in the group treated with OTA and revealed the fragmentation, condensation, and chromatin marginalization of nuclear chromatin, and the shriveled nucleus and chromatin condensation decreased in the inhibitor group compared to the inhibitor-negative group both treated with OTA (Fig. 5C).

These results clearly revealed that the inhibition of *miR-122* can relieve HepG2 cell apoptosis induced by OTA. Consistent with this, the cellular apoptosis of Huh-7 cells transfected with *anti-miR-122* was significantly decreased.⁴²

The inhibitor of *miR-122* downregulated the expression of *miR-122* and elevated *CCNG1* and *Bcl-w* in HepG2 cells treated with OTA

To assess the role of *miR-122* in promoting OTA-induced apoptosis in HepG2 cells, we detected *miR-122* and its target genes after transfecting cells with the *miR-122* inhibitor. We found that the inhibitor caused potent downregulation of *miR-122* (Fig. 6A) ($p < 0.05$). Importantly, the mRNA levels of *CCNG1* and *Bcl-w* were upregulated after the transfection with the inhibitor (Fig. 6B) ($p < 0.05$). Furthermore, the mRNA levels of *p53* and *caspase-3* were both significantly downregulated after the transfection with the inhibitor (Fig. 6C) ($p < 0.05$).

Further, these results showed that *CCNG1/p53* and *Bcl-w/caspase-3* were regulated by *miR-122* to induce the apoptosis of HepG2 cells after OTA treatment.

Experimental

Animals

Male F344 rats (6-7 weeks old) were purchased from Vitalriver (Beijing, China). All of the experimental procedures involving animals were approved by the Ethics Committee of China Agricultural University (permission number: 120020). The rats were fed at the Supervision and Testing Center for GMOs Food Safety, Ministry of Agriculture (Beijing, China). The rats were gavaged with OTA dissolved in corn oil (Aladin, Shanghai, China) at the respective dosage (0, 70 or 210 $\mu\text{g}/\text{kg}$ body weight (b.w.), denoted as C, L, H groups) for 4 or 13 weeks.¹⁶

Cell culture and treatment

HepG2 cells were cultured in high glucose Dulbecco's Modified Eagle's Medium (DMEM), 10% (v/v) fetal bovine serum, 100 U/ml penicillin, 100 U/ml streptomycin at 37 °C in a humidified 5% CO₂ and 95% saturated atmospheric humidity incubator. After HepG2 cells were seeded into plates for 24 h, the cells were treated with OTA. HepG2 cells treated with serum-free medium as a control. After 24 h, the cells were collected for various experiments.

TUNEL assay

TUNEL (Roche, USA) is used to detect apoptotic cells. The liver sections were deparaffinized, rehydrated, washed in PBS and antigen retrieval. The sections were incubated with 0.1 M Tris-HCl (pH 7.5) buffer containing 3% BSA and 20% fetal bovine serum. The TUNEL reaction mixture and the negative control were added. After that, the sections were incubated with DAPI. Digital photographs were taken using a fluorescence microscope.

CCK8 assay

CCK-8 (Beyotime, China) was used to detect HepG2 cell viability. The kit is based on dehydrogenases within the cell that reduce WST-8 to a soluble formazan dye, the accumulation of which was used to analyze cell proliferation and toxicity. The cells were seeded in a 96-well plate. After 24 h, the cells were treated with different concentrations of OTA, then CCK8 was added for incubating. The fluorescence intensity at 450 nm was determined using a microplate reader (thermo, USA).

Hoechst 33342 assay

Hoechst 33342 was used to detect apoptotic HepG2 cells. Hoechst 33342 can combine with the DNA of apoptotic cells. Apoptotic cells appear dark blue. After the cells were seeded for 24 h, the cells were treated with 20 μ M OTA for 24 h and the control cells were treated with serum-free medium. The cells were incubated with Hoechst 33342 in an incubator and kept in the dark. A fluorescence microscope was used to observe the cells.

Flow cytometry analyses of HepG2 cell apoptosis

The apoptosis of HepG2 cells was examined using a FITC-Annexin V/Propidium Iodide (PI) Apoptosis Detection Kit (Kaiji, China). HepG2 cells were seeded into a 6-well plate. Then, they

were treated with OTA. A control was treated with serum-free medium. For flow cytometric analysis, the cells were stained with FITC-Annexin V and PI in the dark. The cells were analyzed using a FACSCalibur flow cytometer (BD Biosciences, USA). For statistical analysis, 20000 total cells per sample were counted.

Real-time PCR analyses of *miR-122* and the target genes

miR-122 was measured using a quantitative real-time PCR Takara Kit. First, total RNA was extracted from the liver tissue and the sample cells using the RNAiso Plus kit (TaKaRa, Dalian, China). *U6* was selected as a control gene for miRNAs expression. The RNA was reversed transcribed into cDNA. The reverse transcription was performed in a DNA Thermal Cycler 4800.

β -actin was used as a control gene for mRNA expression. The cDNA of target genes was synthesized using an oligo(dT) primer. The reaction was carried out in a water bath kettle.

Real-time PCR was performed using an Applied Biosystems 7500 Real-time PCR System (Applied Biosystems, CA). The primers are listed in Table 1, Table 2 and Table 3. The relative expression of each target gene was expressed as $2^{-\Delta\Delta CT}$. All of the experiments were performed in at least triplicate.

***miR-122* inhibitor transfection**

A *hsa-miR-122* inhibitor (5'-UCAAACACCAUUGUCACACUCCA-3') was synthesized by GenePharma (Shanghai, China). NC-inhibitor (5'-CAGUACUUU UGUGUAGUACAA-3') was used as a negative control. HepG2 cells were seeded into plates. Transfection was carried out using HTF (Nuolanxin, China). After 6 h, OTA was added into plates. Then, the cells were harvested for various experiments.

Statistical analysis

The results are expressed as the means \pm standard deviation (SD). The experiments were repeated at least twice, and each experiment was conducted in at least triplicate. The data were subjected to an analysis of variance (ANOVA) or T-test, and the significance was analyzed using the SPSS16.0 software. Differences were considered to be significant when $p < 0.05$.

Conclusion

Our results suggest that OTA induces apoptosis via regulating the expression of *miR-122* and its target genes (Fig. 7). By regulating the expression of *miR-122*, OTA may result in hepatocyte apoptosis through the mitochondrial pathway; Another, OTA induces the hepatocellular carcinoma after long periods of treatment. These findings imply that cell apoptosis is the primary mode of action for OTA-induced hepatotoxicity.

Acknowledgements

This work was funded by “National High Technology Research and Development Program 863 and Laboratory of Food quality and safety, Beijing 100083, China” (Grant No. 2012AA101606). The funders had no role in the study design, data collection and analysis, the decision to publish, or the preparation of the manuscript.

Notes and References

- 1 K. J. van der Merwe, P. S. Steyn, L. Fourie, D. B. Scott and J. J. Theron, *Nature*, 1965. **205**, 1112-3.
- 2 M. Marin-Kuan, S. Nestler, C. Verguet, C. Bezencon, D. Piguat, R. Mansourian, J. Holzwarth, M. Grigorov, T. Delatour, P. Mantle, C. Cavin and B. Schilter, *Toxicol Sci*, 2006. **89**, 120-34.
- 3 D. Mochly-Rosen, M. H. Disatnik and X. Qi, *Rare Dis*, 2014. **2**, e28637.
- 4 R. Valencia-Quintana, J. Sanchez-Alarcon, M. G. Tenorio-Arvide, Y. Deng, J. M. Montiel-Gonzalez, S. Gomez-Arroyo, R. Villalobos-Pietrini, J. Cortes-Eslava, A. R. Flores-Marquez and F. Arenas-Huertero, *Front Microbiol*, 2014. **5**, 102.
- 5 W. Yang, J. Lian, Y. Feng, S. Srinivas, Z. Guo, H. Zhong, Z. Zhuang and S. Wang, *Toxicol Lett*, 2014. **226**, 140-9.
- 6 Q. Dai, J. Zhao, X. Qi, W. Xu, X. He, M. Guo, H. Dweep, W. H. Cheng, Y. Luo, K. Xia, N. Gretz and K. Huang, *BMC Genomics*, 2014. **15**, 333.
- 7 X. Qi, X. Yang, S. Chen, X. He, H. Dweep, M. Guo, W.-H. Cheng, W. Xu, Y. Luo, N. Gretz, Q. Dai and K. Huang, *Scientific Reports*, 2014. **4**.
- 8 Y. Sheng, X. Qi, Y. Liu, M. Guo, S. Chen, X. He, K. Huang and W. Xu, *Food Chem Toxicol*, 2014. **72C**, 242-246.
- 9 M. Girard, E. Jacquemin, A. Munnich, S. Lyonnet and A. Henrion-Caude, *J Hepatol*, 2008. **48**, 648-56.
- 10 A. P. Lewis and C. L. Jopling, *Biochem Soc Trans*, 2010. **38**, 1553-7.
- 11 R. Nassirpour, P. P. Mehta and M. J. Yin, *Plos One*, 2013. **8**.
- 12 L. Gramantieri, M. Ferracin, F. Fornari, A. Veronese, S. Sabbioni, C. G. Liu, G. A. Calin, C. Giovannini, E. Ferrazzi, G. L. Grazi, C. M. Croce, L. Bolondi and M. Negrini, *Cancer Res*, 2007. **67**, 6092-9.
- 13 F. Fornari, L. Gramantieri, C. Giovannini, A. Veronese, M. Ferracin, S. Sabbioni, G. A. Calin, G. L. Grazi, C. M. Croce, S. Tavolari, P. Chieco, M. Negrini and L. Bolondi, *Cancer Res*, 2009. **69**, 5761-7.
- 14 B. K. Elamin, E. Callegari, L. Gramantieri, S. Sabbioni and M. Negrini, *Mutat Res*, 2011. **717**, 67-76.
- 15 C. J. Lin, H. Y. Gong, H. C. Tseng, W. L. Wang and J. L. Wu, *Biochem Biophys Res Commun*, 2008. **375**, 315-20.
- 16 J. Cui, T. Wei, L. N. Liu, X. Zhang, X. Qi, Z. F. Zhang and Z. Q. Wang, *Parasitol Res*, 2014. **113**, 3511-6.
- 17 E. Essid and E. Petzinger, *Mycotoxin Res*, 2011. **27**, 167-76.
- 18 M. Chopra, P. Link, C. Michels and D. Schrenk, *Cell Biol Toxicol*, 2010. **26**, 239-54.
- 19 G. B. E. El, A. Rodriguez-Enfedaque, C. Bouaziz, M. Ladjimi, F. Renaud and H. Bacha, *J Biochem Mol Toxicol*, 2009. **23**, 87-96.
- 20 H. Kutay, S. Bai, J. Datta, T. Motiwala, I. Pogribny, W. Frankel, S. T. Jacob and K. Ghoshal, *J Cell Biochem*, 2006. **99**, 671-8.
- 21 J. Burchard, C. Zhang, A. M. Liu, R. T. Poon, N. P. Lee, K. F. Wong, P. C. Sham, B. Y. Lam, M. D. Ferguson, G. Tokiwa, R. Smith, B. Leeson, R. Beard, J. R. Lamb, L. Lim, M. Mao, H. Dai and J. M. Luk, *Mol Syst Biol*, 2010. **6**, 402.
- 22 O. Cheung, P. Puri, C. Eicken, M. J. Contos, F. Mirshahi, J. W. Maher, J. M. Kellum, H. Min,

- V. A. Luketic and A. J. Sanyal, *Hepatology*, 2008. **48**, 1810-20.
- 23 L. Ma, J. Liu, J. Shen, L. Liu, J. Wu, W. Li, J. Luo, Q. Chen and C. Qian, *Cancer Biol Ther*, 2010. **9**, 554-61.
- 24 X. Huang, F. Huang, D. Yang, F. Dong, X. Shi, H. Wang, X. Zhou, S. Wang and S. Dai, *J Cell Mol Med*, 2012. **16**, 2637-46.
- 25 J. Xu, X. M. Zhu, L. J. Wu, R. Yang, Z. R. Yang, Q. F. Wang and F. S. Wu, *Liver International*, 2012. **32**, 752-760.
- 26 J. H. Lian, W. H. Wang, J. Q. Wang, Y. H. Zhang and Y. Li, *Asian Pac J Cancer Prev*, 2013. **14**, 5017-21.
- 27 W. Hou, T. N. Bukong, K. Kodys and G. Szabo, *Alcohol Clin Exp Res*, 2013. **37**, 599-608.
- 28 T. Ohtsuka, H. Ryu, Y. A. Minamishima, A. Ryo and S. W. Lee, *Oncogene*, 2003. **22**, 1678-87.
- 29 S. F. Wang, L. P. Qiu, X. L. Yan, W. S. Jin, Y. Z. Wang, L. Z. Chen, E. J. Wu, X. Ye, G. F. Gao, F. S. Wang, Y. Chen, Z. P. Duan and S. D. Meng, *Hepatology*, 2012. **55**, 730-741.
- 30 M. B. Kastan, C. E. Canman and C. J. Leonard, *Cancer Metastasis Rev*, 1995. **14**, 3-15.
- 31 M. V. Kato, *Leuk Lymphoma*, 1999. **33**, 181-6.
- 32 V. Manfe, E. Biskup, A. Rosbjerg, M. Kamstrup, A. G. Skov, C. M. Lerche, B. T. Lauenborg, N. Odum and R. Gniadecki, *PLoS One*, 2012. **7**, e29541.
- 33 J. Cui, J. Liu, S. Wu, Y. Wang, H. Shen, L. Xing, J. Wang, X. Yan and X. Zhang, *Arch Toxicol*, 2013. **87**, 1829-40.
- 34 W. C. Tsai, S. D. Hsu, C. S. Hsu, T. C. Lai, S. J. Chen, R. Shen, Y. Huang, H. C. Chen, C. H. Lee, T. F. Tsai, M. T. Hsu, J. C. Wu, H. D. Huang, M. S. Shiao, M. Hsiao and A. P. Tsou, *J Clin Invest*, 2012. **122**, 2884-97.
- 35 J. Folch, D. Alvira, M. Lopez-Querol, M. Tajés, F. X. Sureda, A. Forsby, V. Rimbau, A. Camins and M. Pallas, *Toxicol In Vitro*, 2010. **24**, 465-71.
- 36 B. Antonsson, *Cell Tissue Res*, 2001. **306**, 347-61.
- 37 X. Zhang, C. Boesch-Saadatmandi, Y. Lou, S. Wolfram, P. Huebbe and G. Rimbach, *Genes Nutr*, 2009. **4**, 41-8.
- 38 Z. N. Li, X. H. Zhang, J. F. Cui and W. J. Kang, *Journal of Biochemical and Molecular Toxicology*, 2012. **26**, 139-146.
- 39 X. L. Shen, B. Zhang, R. Liang, W. H. Cheng, W. Xu, Y. Luo, C. Zhao and K. Huang, *Food Chem Toxicol*, 2014. **69**, 202-9.
- 40 Q. L. Deveraux, R. Takahashi, G. S. Salvesen and J. C. Reed, *Nature*, 1997. **388**, 300-4.
- 41 Q. L. Deveraux, N. Roy, H. R. Stennicke, T. Van Arsdale, Q. Zhou, S. M. Srinivasula, E. S. Alnemri, G. S. Salvesen and J. C. Reed, *EMBO J*, 1998. **17**, 2215-23.
- 42 X. Wu, S. Q. Wu, L. Tong, T. A. Luan, L. X. Lin, S. L. Lu, W. R. Zhao, Q. Q. Ma, H. M. Liu and Z. H. Zhong, *Scandinavian Journal of Gastroenterology*, 2009. **44**, 1332-1339.

Figure legends

Fig. 1 Hepatocyte apoptosis. (A) The liver sections of rats treated with OTA for 4 weeks. (B) The liver sections of rats treated with OTA for 13 weeks. Arrowheads indicate hepatocyte apoptosis. N: negative group; C: control group; L: low-dose group; H: high-dose group. Original magnification = 200 ×.

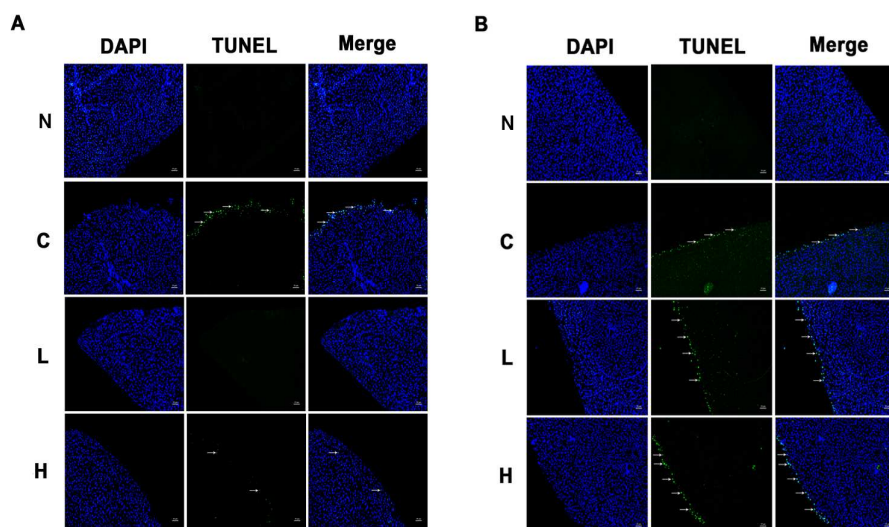
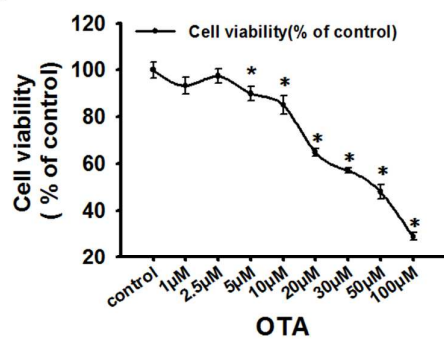
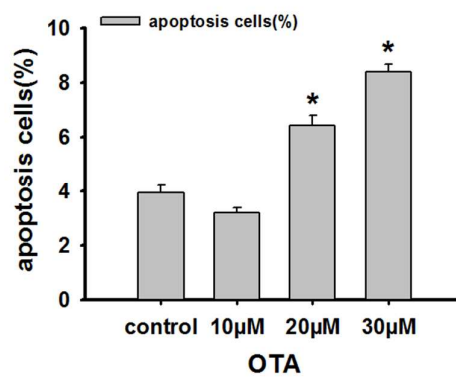
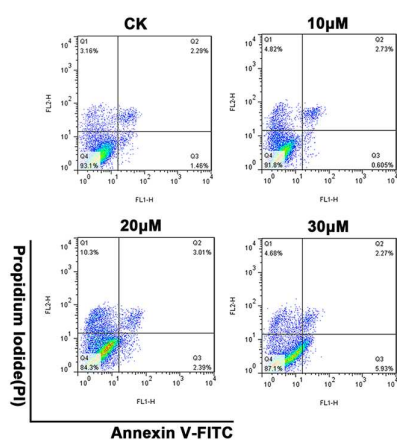


Fig. 2 Cytotoxicity of OTA. (A) The effect of various concentrations of OTA on cell viability was measured using a CCK-8 assay. (B) The apoptosis of cells treated with different concentrations of OTA was measured using flow cytometry. (C) Hoechst 33342 nuclear staining showed the acceleration of chromatin condensation in HepG2 cells. Arrowheads indicate chromatin condensation consistent with the occurrence of apoptosis. Original magnification = 200 ×. The data are presented as the mean ± SD of three independent experiments. * $p < 0.05$ compared with control group.

A



B



C

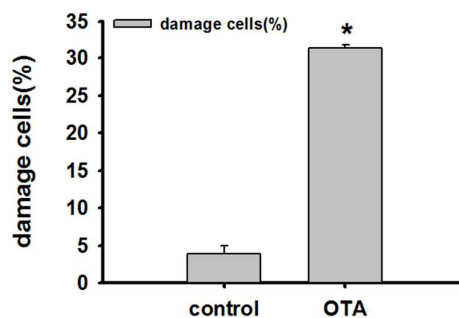
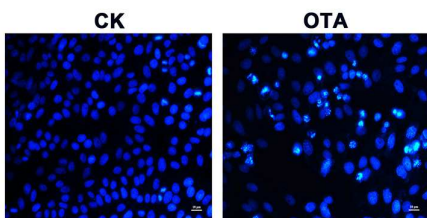


Fig. 3 Changes in the expression levels of *miR-122* in the livers of male rats and HepG2 cells treated with OTA. C: control group; L: low-dose group; H: high-dose group. The data are presented as the mean \pm SD of $n=6$ *in vivo* and three independent experiments *in vitro*. $*p < 0.05$ compared with control group.

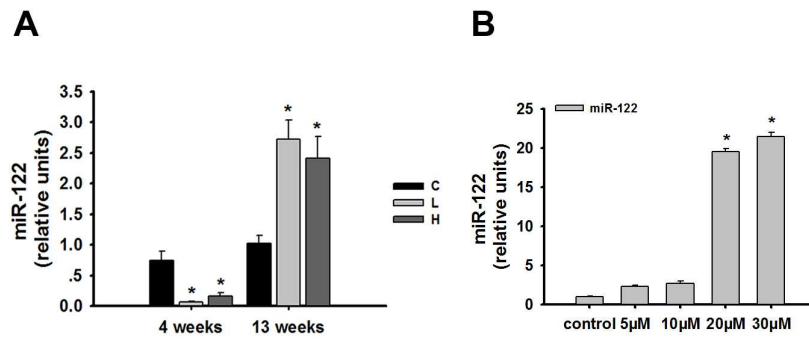


Fig. 4 The expression of the mRNAs of *CCNG1*, *Bcl-w*, *p53* and *caspase-3* in the liver and HepG2 cells treated with OTA. C: control group; L: low-dose group; H: high-dose group. The data are presented as the mean \pm SD of $n=6$ *in vivo* and three independent experiments *in vitro*. $*p < 0.05$ compared with control group.

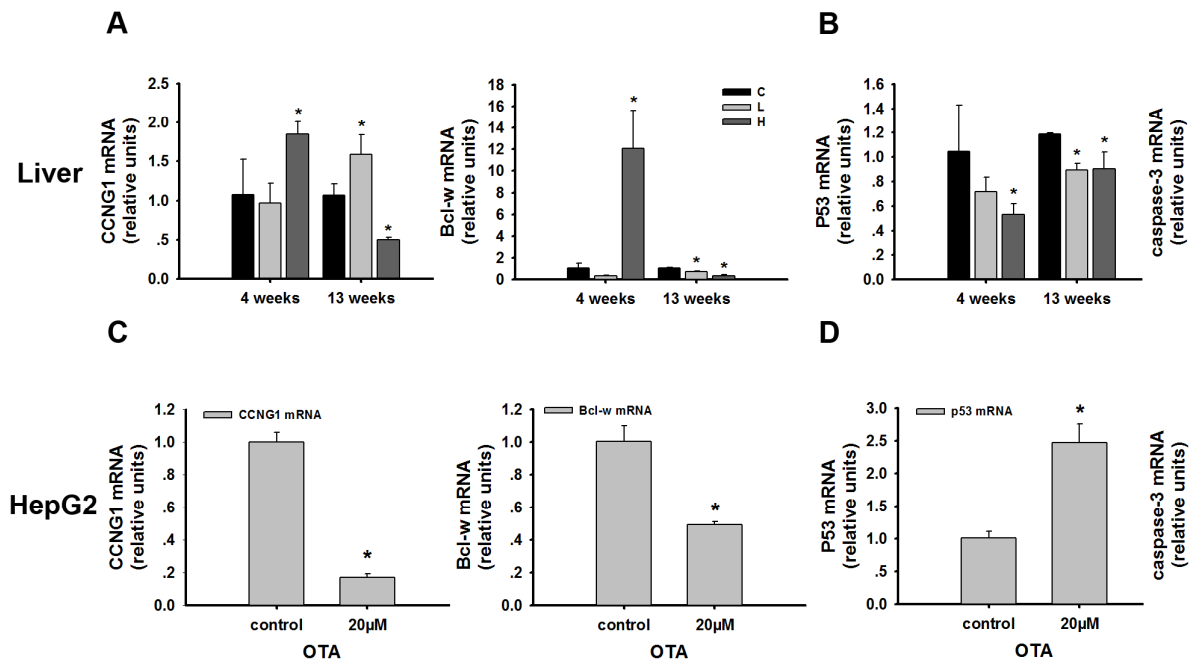


Fig. 5 Mitigation of the cytotoxicity of OTA. HepG2 cells were incubated with OTA or serum-free medium after being transfected with an NC-inhibitor or *hsa-miR-122* inhibitor. (A) The inhibition effect of various concentrations of *hsa-miR-122* inhibitor was measured using real-time PCR. $*p < 0.05$ compared with control group. (B) The apoptosis of HepG2 cells were measured using flow cytometry. $*p < 0.05$ compared with NC+OTA group. (C) The changes in the acceleration of chromatin condensation in HepG2 cells were detected using Hoechst 33342 staining. The arrowheads indicate chromatin condensation. Original magnification = 200 \times . The data are presented as the mean \pm SD of three independent experiments. $*p < 0.05$ compared with NC+OTA group.

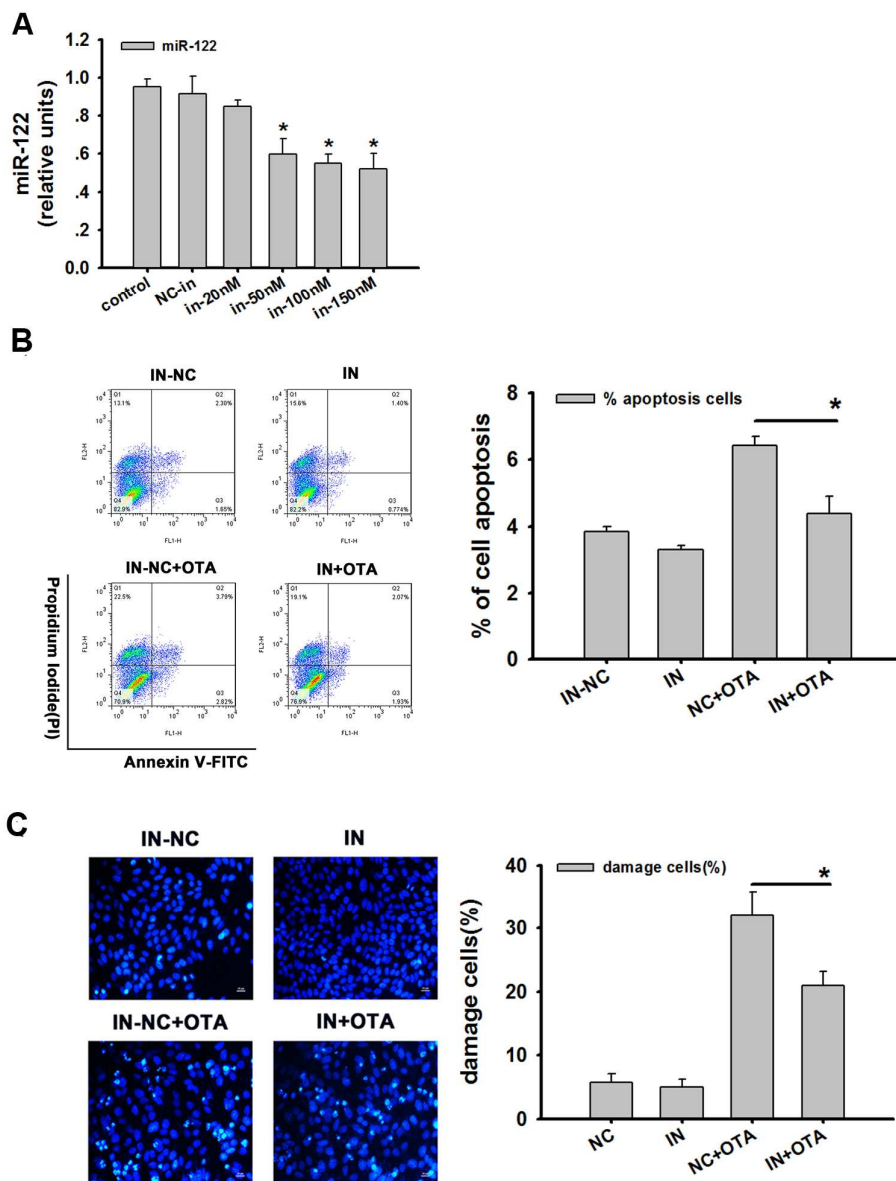


Fig. 6 The expression of *miR-122* and the mRNAs of *CCNG1*, *Bcl-w*, *p53* and *caspase-3* in HepG2 cells treated with 20 μ M OTA or serum-free medium after being transfected with an NC-inhibitor or *hsa-miR-122*. The data are presented as the mean \pm SD of three independent experiments. (A) The first $*p < 0.05$ compared with control group. The second $*p < 0.05$ compared with OTA group. (B) $*p < 0.05$ compared with NC+OTA group. (C) $*p < 0.05$ compared with NC+ OTA group.

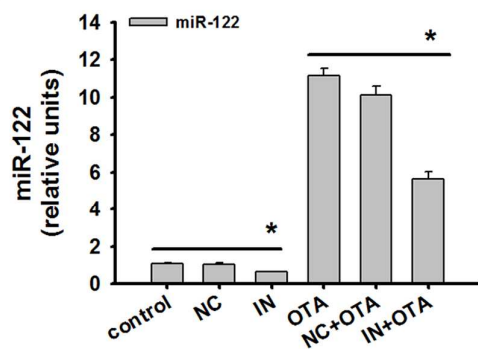
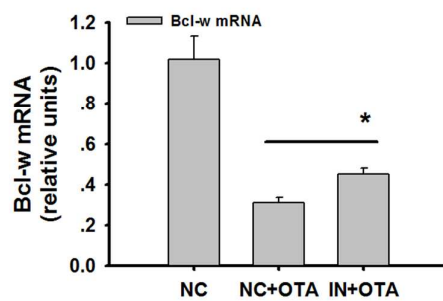
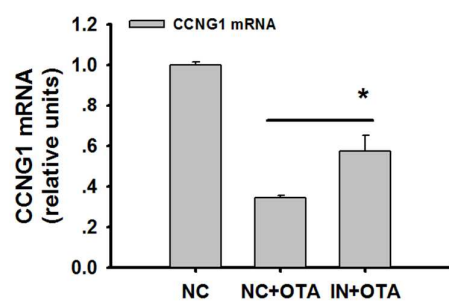
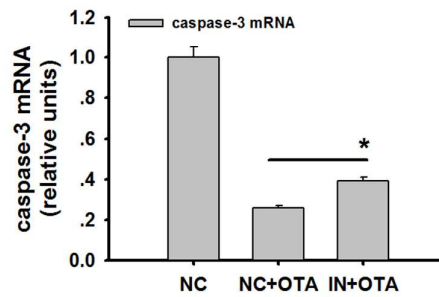
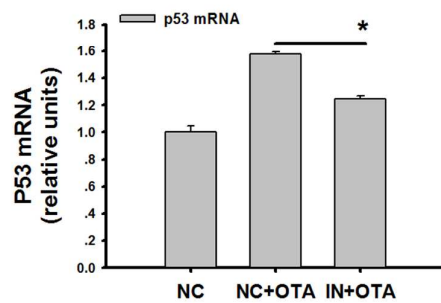
A**B****C**

Fig. 7 A model for the role of *miR-122* in Ochratoxin A-induced hepatocyte apoptosis *in vivo* and *in vitro*.

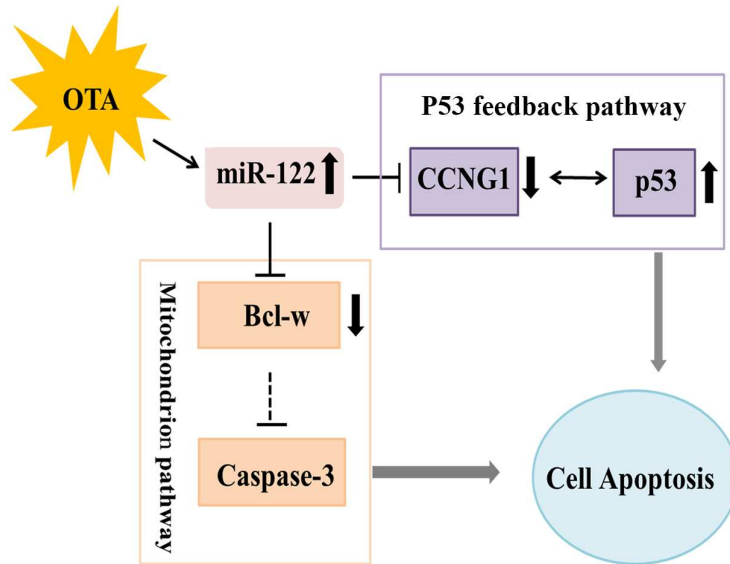


Table 1 Primer sequences of genes used for qRT-PCR.

Gene name	RT-primer
<i>miR-122-RT</i>	CTCAACTGGTGTCGTGGAGTCGGCAATTCAGTTGAGCAAACACC
<i>U6-RT</i>	AACGCTTCACGAATTTGCGT

Table 2 Primer sequences of miRNAs used for qRT-PCR

Gene name	Forward primer	Reverse primer
<i>miR-122</i>	ATCGACATCTGGAGTGTGACAAT G	CTCAACTGGTGTTCGTGGAGTC
<i>U6</i>	CTCGCTTCGGCAGCACA	AACGCTTCACGAATTTGCGT

Table 3 Primer sequences of genes used for qRT-PCR.

Gene name	Forward primer	Reverse primer
<i>rat-CCNG1</i>	CTCTGTGGCAGTTGGGCTAA	AACAGCTAACGTGGTGAGGG
<i>rat-p53</i>	GTCGGCTCCGACTATACCACTATC	CTCTCTTTGCACTCCCTGGGGG
<i>rat-Bcl-w</i>	CACCCAGGTCTCCGATGAAC	TTGTTGACACTCTCAGCACAC
<i>rat-Caspase3</i>	CTGGACTGCGGTATTGAGAC	CCGGGTGCGGTAGAGTAAGC
<i>hsa-CCNG1</i>	AGCTGCAGTCTCTGTCAAG	ATGTCTCTGTGTCAAAGCCA
<i>hsa-p53</i>	TAACAGTTCCTGCATGGGCGGC	AGGACAGGCACAAACACGCA CC
<i>hsa-Bcl-w</i>	CACCCAGGTCTCCGATGAAC	TTGTTGACACTCTCAGCACAC
<i>hsa-Caspase3</i>	CTCCTTCCATCAAATAGAAC	AATTAACAATCATTGCCTCT
<i>rat-β-actin</i>	CCCATCTATGAGGGTTACGC	TTTAATGTCACGCACGATTTC
<i>hsa-β-actin</i>	TCGTGCGTGACATTAAGGAG	AGGAAGGAAGGCTGGAAGAG